Title

Wound-induced Ca2+ wave propagates through a simple release and diffusion mechanism

Journal

Molecular Biology of the Cell, 28(11)

ISSN

1059-1524

Authors

Handly, L Naomi
Wollman, Roy

Publication Date

2017-06-01

DOI

10.1091/mbc.e16-10-0695

Peer reviewed

Wound-induced Ca^{2+} wave propagates through a simple release and diffusion mechanism

L. Naomi Handly[a,b] and Roy Wollman[a,b,c,*]
[a]Department of Chemistry and Biochemistry, [b]Institute for Quantitative and Computational Biosciences, and
[c]Department of Integrative Biology and Physiology, University of California, Los Angeles, Los Angeles, CA 90095

ABSTRACT **Damage-associated molecular patterns (DAMPs) are critical mediators of information concerning tissue damage from damaged cells to neighboring healthy cells. ATP acts as an effective DAMP when released into extracellular space from damaged cells. Extracellular ATP receptors monitor tissue damage and activate a Ca^{2+} wave in the surrounding healthy cells. How the Ca^{2+} wave propagates through cells after a wound is unclear. Ca^{2+} wave activation can occur extracellularly via external receptors or intracellularly through GAP junctions. Three potential mechanisms to propagate the Ca^{2+} wave are source and sink, amplifying wave, and release and diffusion. Both source and sink and amplifying wave regulate ATP levels using hydrolysis or secretion, respectively, whereas release and diffusion relies on dilution. Here we systematically test these hypotheses using a microfluidics assay to mechanically wound an epithelial monolayer in combination with direct manipulation of ATP hydrolysis and release. We show that a release and diffusion model sufficiently explains Ca^{2+}-wave propagation after an epithelial wound. A release and diffusion model combines the benefits of fast activation at short length scales with a self-limiting response to prevent unnecessary inflammatory responses harmful to the organism.**

Monitoring Editor
Alex Mogilner
New York University

Received: Oct 4, 2016
Revised: Apr 7, 2017
Accepted: Apr 7, 2017

INTRODUCTION

The epithelium provides a key protective layer that isolates the internal environment of an organism from outside pathogens. A temporary loss of the epithelial barrier caused by wounds places an organism in a precarious and vulnerable situation (Enyedi and Niethammer, 2015). A timely defense and healing program is vital for organism survival. Wound-healing response requires the coordinated action of multiple cell types (Sonnemann and Bement, 2011). Neutrophil cells infiltrate the wounded area to proactively defend against infection. Phagocytosis of pathogens and necrotic cells requires macrophage recruitment. Fibroblasts increase extracellular matrix secretion and provide contractile forces. Finally, epithelial cells proliferate and migrate to close the wound. A plethora of cytokine mediators secreted by the different cell types participating in the wound response regulate the complex wound-healing program. However, cytokine secretion, which often requires de novo expression, occurs on an hour time scale (Sonnemann and Bement, 2011; Cordeiro and Jacinto, 2013). The sensitive state of the wounded epithelium requires that wound healing begin as soon as the wound occurs. Therefore cytokine secretion is too slow to act as the initial signal that activates wound-healing programs. A timely wound-healing response necessitates a transcriptionally independent program to propagate information regarding the wound to neighboring healthy cells.

Damage-associated molecular patterns (DAMPs) are composed of a set of chemical ligands that are released from cells upon physical damage (Cordeiro and Jacinto, 2013). DAMPs provide the first indication of damage and are used to activate transcriptionally independent programs. DAMPs quickly propagate information regarding the wound to notify healthy cells surrounding the wound that cellular damage has occurred. Potentially, the gradients formed by DAMPs provide neighboring cells with positional information concerning how far they are from the wound (Sonnemann and Bement, 2011). These damage signals include Ca^{2+} waves, reactive oxygen species, and purinergic molecules such as ATP (Cordeiro and Jacinto, 2013).

Although best known for its key role in cellular metabolism, there has been a growing appreciation for an additional role of ATP as a

This article was published online ahead of print in MBoC in Press (http://www.molbiolcell.org/cgi/doi/10.1091/mbc.E16-10-0695) on April 12, 2017.

*Address correspondence to: Roy Wollman (rwollman@ucla.edu).

Abbreviations used: DAMP, damage-associated molecular pattern; ER, endoplasmic reticulum.

Supplemental Material can be found at:
http://www.molbiolcell.org/content/suppl/2017/04/10/mbc.E16-10-0695v1.DC1

paracrine signaling molecule (Schwiebert and Zsembery, 2003). Under normal physiological conditions, extracellular ATP levels are typically ~1 nM—six orders of magnitude less than cytoplasmic ATP levels of ~1 mM (Corriden and Insel, 2010). This large gradient, actively maintained by cells, makes ATP a powerful damage indicator, as any loss of membrane integrity causes an immediate increase in extracellular ATP. Furthermore, previous work has demonstrated that ATP is a key initial signaling molecule required for activation of epithelial wound response (Feldman, 1991; Caporossi and Manetti, 1992; Pastor and Calonge, 1992).

ATP released from cells after a mechanical wound initiates a Ca^{2+} wave that propagates from the wound in an isotropic pattern.

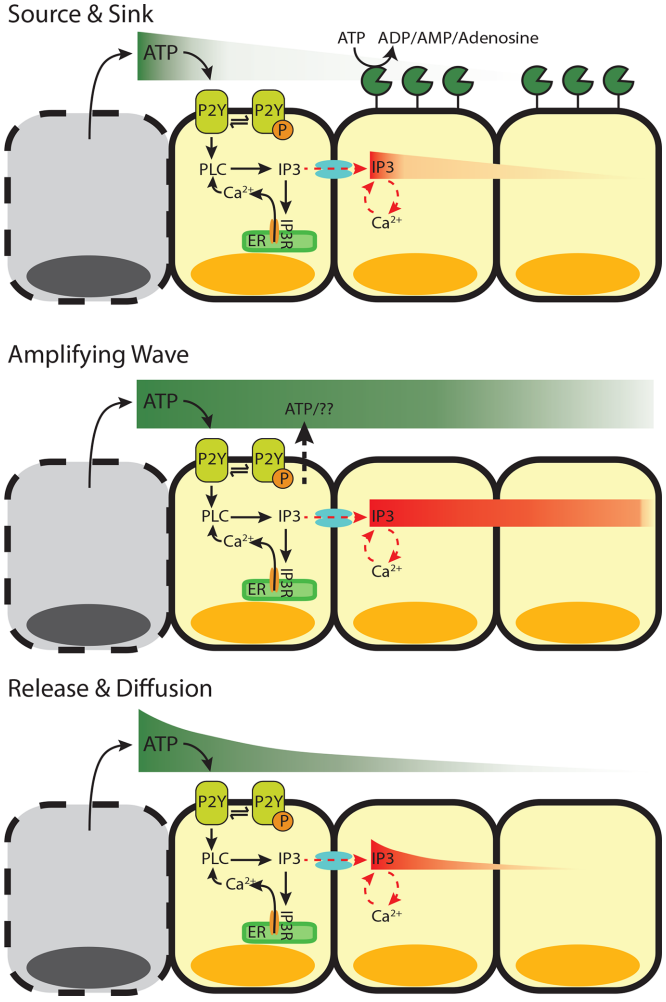

FIGURE 1: Ca^{2+}-wave propagation after wounding. After wounding, cytosolic Ca^{2+} levels increase in the surrounding healthy cells in a wave-like manner. Ca^{2+} can be activated in cells either extracellularly (ATP binding to extracellular receptors) or intracellularly (IP3 traveling between cells). However, the Ca^{2+} wave can propagate using different mechanisms. 1) Source and sink (top). After the initial release of ATP from wounded cells (source), which activates the cells immediately surrounding the wound, the remaining activating molecules (either ATP or IP3) are hydrolyzed (sink) as they move away from the wounded area and activate neighboring cells. 2) Amplifying wave (middle). In this active mechanism, ATP-induced ATP release continues to propagate ATP and IP3 molecules to activate neighboring cells at faraway distances. 3) Release and diffusion (bottom). The release of ATP from wounded cells diffuses away from the wound source to activate neighboring cells, with little to no regulation.

Initially, ATP released from wounded cells binds to P2Y receptors on surrounding healthy cells to increase cytoplasmic Ca^{2+} levels (Figure 1). More precisely, phosphorylation of P2Y by ATP activates phospholipase C (PLC) to catalyze the degradation of phosphatidylinositol 4,5-bisphosphate (PIP2) to inositol triphosphate (IP3) and diacyl glycerol (DAG) (Berridge *et al.*, 2000; Bootman, 2012). IP3 then binds to IP3R on the endoplasmic reticulum (ER) to release Ca^{2+} stores into the cytoplasm. IP3 can pass between cells through connexin channels, resulting in intracellular Ca^{2+} activation (Höfer *et al.*, 2001; Warren *et al.*, 2010; Sun *et al.*, 2012; Razzell *et al.*, 2013). Although the intracellular pathways that connect extracellular ATP to activate Ca^{2+} signaling have been carefully elucidated (Dupont, 2014), the tissue-level pathways responsible for forming the Ca^{2+} wave remain unclear.

Like other DAMPs, ATP may provide positional information for healthy cells surrounding a wound. Handly *et al.* (2015) found that ATP-activated extracellular signal-regulated kinase transactivation maximizes positional information by locally averaging the epidermal growth factor (EGF) signal using paracrine communication. However, the spatiotemporal propagation of ATP after a wound to provide positional information is not fully understood. Several models have been proposed to explain how neighboring cells are notified of damage after passive release of ATP from damaged cells (Figure 1). In the first model, source and sink, ectonucleotidases such as NTPDase2 quickly hydrolyze ATP (Locovei *et al.*, 2006; Ho *et al.*, 2013). In the second model, amplifying wave, active propagation mechanisms increase the concentration of extracellular ATP. Specifically, it has been proposed that cells exposed to extracellular ATP respond by actively secreting ATP through pannexin-1 channels (Locovei *et al.*, 2006; Dubyak, 2009; Corriden and Insel, 2010; Junger, 2011). In the third model, release and diffusion, simple diffusion and dilution of the initial ATP signal control Ca^{2+}-wave propagation. Although molecular studies show support for each model, uncertainty remains concerning which mechanism is primarily responsible for propagating the ATP-induced Ca^{2+} wave. Here we use a novel wounding device to mechanically wound an epithelial monolayer (Handly *et al.*, 2015). Using single-cell wound data combined with genetic and pharmaceutical manipulations, we identify the underlying mechanism responsible for the spread of extracellular ATP in a mechanically wounded epithelial monolayer.

RESULTS

Mechanical wounds initiate a Ca^{2+} wave that scales with wound size

Measuring the spatial cellular wound response requires the ability to wound an epithelial monolayer in a convection-free environment. We developed a novel microfluidics wounding device to mechanically wound an epithelial monolayer (Figure 2A; Handly *et al.*, 2015). Our wounding device has two layers: a bottom cell layer and a top air layer. Cells in the cell chamber are mechanically wounded by a pillar in the ceiling of the cell layer when air pressure is increased in the air layer (Figure 2B). Flow is blocked during wounding to prevent any convection within the device from creating an isotropic Ca^{2+} wound response (Figure 2C). One advantage of our wounding device over conventional wounding methods such as scratch assays is the ability to create reproducible wounds (Figure 2D). Reproducible wounding is imperative to measure the spatial response to ensure that each wound elicits a similar response from the surrounding healthy cells.

The isotropic cellular Ca^{2+} response to wounding contains a spatial response that scales with wound size. When measuring the Ca^{2+} response to mechanical wounds, we found that the fraction of responding cells decreased with increasing distance from the

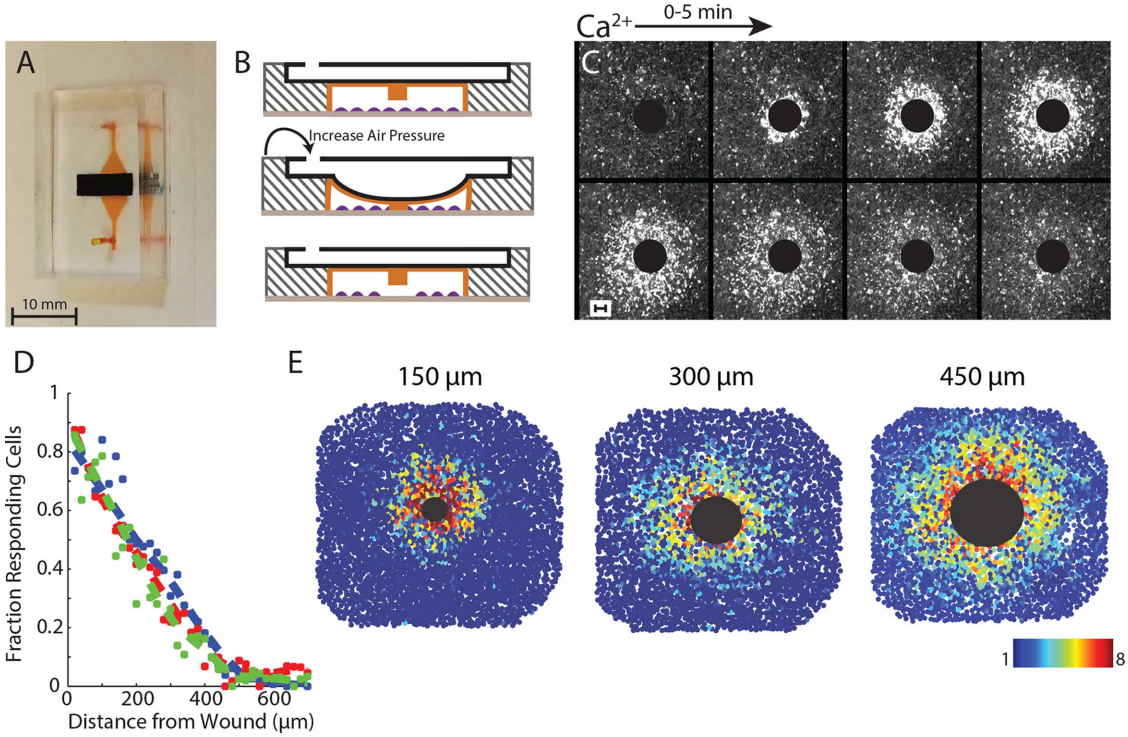

FIGURE 2: Measuring the Ca^{2+} wave using a microfluidics wounding device. (A) Dual-layer microfluidics device with cell chamber (orange) and air channel (black). (B) Cells (purple) cultured in the cell chamber (orange) are mechanically wounded when a PDMS pillar in the ceiling of the cell chamber is lowered when air pressure is increased in the air layer (black). (C) Ca^{2+} activation in MCF-10A cells after a 300-μm-diameter wound. Black circle represents the wounded area. Images are over a period of 5 min. Cytosolic Ca^{2+} level indicated by Fluo-4 AM. (D) Fraction of responding cells across the healthy surrounding cells decreases with increasing distance from the wound. Dashed lines represent the best fit for three different 300-μm wounds. (E) The Ca^{2+} wave scales with increasing wound size. The large black circle represents the wounded area according to the size of the wound (150-, 300-, and 450-μm-diameter wounds). Colored circles represent fold maximum Ca^{2+} increase for a single cell as indicated by the color bar. Ca^{2+} increase is indicated by Fluo-4 AM dye.

wound (Figure 2D). In addition, this response scales with wound size (Figure 2E and Supplemental Figure S1). Spatial information, or knowing where you are in relation to the wound, is imperative during wound healing to ensure that each cell responds appropriately. For Ca^{2+} response, we find that cells further from the wound have a smaller and slower response than cells closer to the wound. Although there are biological processes in place, such as paracrine averaging, to ensure that each cell generates the appropriate response based on its position (Handly *et al.*, 2015), we wondered how the initial Ca^{2+} gradient forms in an epithelial monolayer after a wound.

ATP is released in response to mechanical wounding and is required for wound closure

ATP released from wounded epithelial cells is a key damage indicator in the initial wound response (Feldman, 1991; Caporossi and Manetti, 1992; Pastor and Calonge, 1992). We examined whether a monolayer of MCF-10A cells, a breast mammary epithelial line, requires ATP release to heal mechanical wounds made by our wounding device. We first established whether initial ATP release is required for a Ca^{2+} response. Indeed, the addition of the ATP scavenger apyrase prevented a gradient of Ca^{2+} activation in cells surrounding the wound (Figure 3A and Supplemental Figure S1). Next we determined whether the initial ATP released from wounded cells is necessary to the overall wound-healing response. Epithelial cells migrate and proliferate in order to close the wound. Other work has shown that epithelial cells simply sense empty space in order to proliferate and migrate into the wounded area (Block *et al.*, 2004; Klarlund and Block, 2011). However, unlike what happens in a scratch assay, wounded cells tend to remain in the wounded area from our wounding device. Wounding MCF-10A cells in the presence of apyrase prevents cells from migrating into the wounded area (Figure 3, B and C). This lack of migration in the presence of apyrase agrees with previous wound studies (Wesley *et al.*, 2007; Gault *et al.*, 2014; Nakagawa *et al.*, 2014; Takada *et al.*, 2014). Overall we find that the initial release of ATP is required for Ca^{2+} activation, as well as for epithelial wound closure.

The Ca^{2+} wave propagates by extracellular activation

The wave of Ca^{2+} activation after wounding can spread using extracellular or intracellular stimulus. Previous data indicate that the Ca^{2+} response after wounding depends on the DAMP ATP (Klepeis *et al.*, 2001, 2004; Yin *et al.*, 2007; Block and Klarlund, 2008; Cordeiro and Jacinto, 2013; Figure 3). ATP initially released from damaged cells binds to extracellular receptors on neighboring cells, causing a cytosolic Ca^{2+} increase within that cell. From here, the propagation of Ca^{2+} activation in neighboring cells can occur via extracellular or intracellular mechanisms. Extracellular stimulation results from ATP propagation that can be augmented by either active release of ATP from cells or degradation by nucleotidases (Locovei *et al.*, 2006; Ho *et al.*, 2013). Intracellular stimulation occurs when IP3 travels

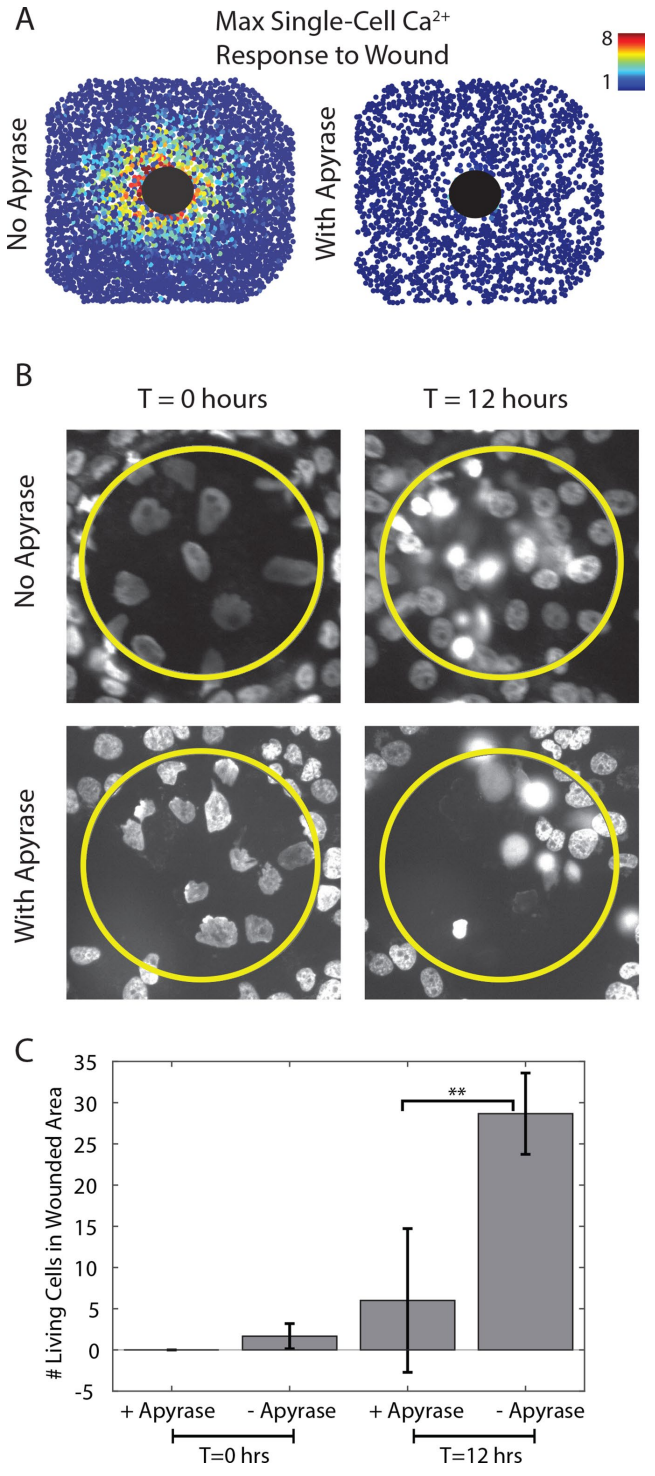

FIGURE 3: Cell migration after a wound requires ATP. (A) Maximum Ca^{2+} projection indicated by Fluo-4 AM after a 300-μm-diameter wound in the absence (left) and presence (right) of the ATP scavenger apyrase (5 U per wounding device). Each circle represents the fold maximum Ca^{2+} increase of a single cell as indicated by the color bar. The large black circle represents the wounded area. Mechanical wounding generates a Ca^{2+} response gradient surrounding the wound. Apyrase inhibits this response. (B) Nuclei with Hoechst staining after a 150-μm-diameter wound in the absence (top) and presence (bottom) of the ATP scavenger apyrase (5 U per wounding device). The yellow circle represents the wounded area, and *T* is the time after the wound. Surrounding healthy cells migrate into the wounded area in the absence of apyrase in 12 h. No migration is seen after wounding in the presence of apyrase. (C) Quantification of B. The number of living cells in the wounded area is significantly higher (**$p < 0.05$, *t* test, $n = 3$ wounds) in the absence of apyrase 12 h after a wound compared with a wound in the presence of apyrase.

between cells via GAP junctions to bind to IP3 receptor to release internal Ca^{2+} stores cells in neighboring cells (Höfer *et al.*, 2001; Warren *et al.*, 2010; Sun *et al.*, 2012; Razzell *et al.*, 2013). In intracellular stimulation, ATP released from wounded cells activates the initial Ca^{2+} response in healthy cells immediately surrounding a wound. GAP junctions then propagate the spread of Ca^{2+} activation to cells further from the wound. We first determined whether the Ca^{2+} wave propagates internally or externally.

To determine whether the spread of the Ca^{2+} wave is activated through intracellular or extracellular mechanisms, we used our novel wounding device to wound cells in the presence and absence of flow. Based on our previous data (Figure 2), we found that the Ca^{2+} wave travels isotropically from the wound in the absence of flow. We wondered whether the response would maintain an isotropic pattern if cells were wounded in the presence of flow. If flow has no influence on the shape of the response, then the Ca^{2+} wave most likely propagates internally, where it is not influenced by extracellular flow. When wounding in the presence of flow, however, we found that the response propagates in the direction of the flow (Figure 4A and Supplemental Figure S1). This indicates that Ca^{2+} wave propagation is not independent of the extracellular environment.

We used a synthetic G protein–coupled receptor designer receptor exclusively activated by designer drug (DREADD) that is activated by the small molecule clozapine-*N*-oxide (CNO) to further investigate whether Ca^{2+} response propagates intracellularly or extracellularly by activating a Ca^{2+} response without ATP in a single cell and watching the surrounding cells in a nonwound setting (Armbruster *et al.*, 2007; Dong *et al.*, 2010). By activating a Ca^{2+} response without a wound, we ensured that there are no artifacts created by flow during Ca^{2+}-wave propagation. We used a DREADD that uses Gq-mediated signaling to ensure that Ca^{2+} is activated in cells using the same signaling mechanism as the ATP-activated Ca^{2+} response. To determine whether the Ca^{2+} wave travels internally, we cocultured both DREADD-expressing and -nonexpressing cells such that DREADD-expressing cells are surrounded by nonexpressing cells (Figure 4B). The addition of CNO activates a Ca^{2+} response in DREADD-expressing cells. Whether the Ca^{2+} wave travels internally or externally is indicated by whether the surrounding nonexpressing cells also show an increase in Ca^{2+}. A Ca^{2+} response in the surrounding nonexpressing cells would indicate an internal propagation mechanism of the Ca^{2+} wave. However, if the wave depends on extracellular stimulus, then only the DREADD-expressing cells will respond. We found that upon the addition of CNO, only DREADD-expressing cells respond (Figure 4C and Supplemental Figure S2). Taken together, these pieces of evidence indicate that the Ca^{2+} wave travels extracellularly.

Source and sink: extracellular ATP degradation does not affect Ca^{2+} activation

In the source and sink model, ATP hydrolysis dominates ATP propagation. Here the lifetime of an ATP molecule determines how long and far it will diffuse from the wound source. Ectonucleotidases present on the plasma membrane metabolize ATP to ADP, AMP, or

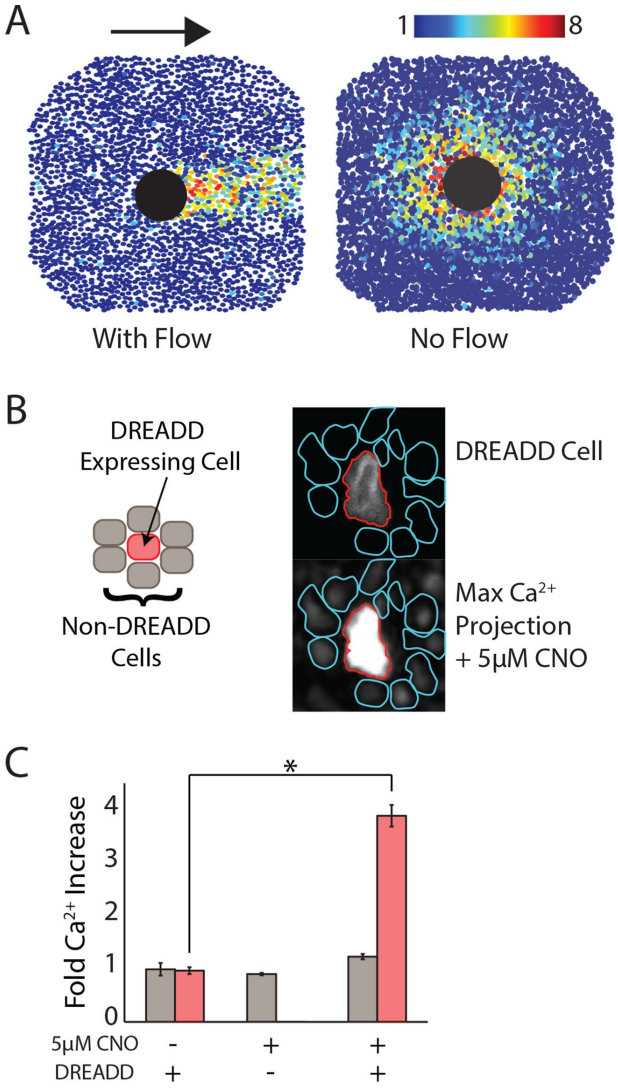

FIGURE 4: Ca^{2+}-wave spread requires extracellular activation. All Ca^{2+} is indicated by Fluo-4 AM dye. (A) When flow is present during the wound, the Ca^{2+} wave goes in the direction of the flow (left). When flow is blocked, the Ca^{2+} wave propagates in an isotropic manner (right). The large black circle represents the wounded area, and colored circles represent fold maximum Ca^{2+} increase for a single cell as indicated by the color bar. Arrow indicates direction of flow. (B) Left, DREADD-expressing (red) and -nonexpressing (gray) MCF-10A cells are cocultured such that each DREADD-expressing cell is surrounded by nonexpressing cells. Right, on addition of 5 μM CNO, the DREADD cell shows Ca^{2+} activation, but the surrounding, nonexpressing cells do not (DREADD cell in red; surrounding, nonexpressing cells in cyan). Top, expression of mCherry in DREADD cells; bottom, maximum Ca^{2+} projection after addition of 5 μM CNO as indicated by Fluo-4 AM. (C) Quantification of B. DREADD-expressing cells in red; nonexpressing cells in gray. Only DREADD-expressing cells have Ca^{2+} increase after the addition of 5μM CNO. Error bars indicate SEM; $n = 3$; *$p < 0.005$, *t* test.

adenosine (Idzko *et al.*, 2014). The degradation of ATP released from wounded cells can lead to the formation of the Ca^{2+}-wave gradient. In this case, each subsequent cell receives a lower dose of ATP, resulting in a lower magnitude of Ca^{2+} activation in a cell. We used pharmaceutical manipulation to determine the role of ATP degradation in creating the Ca^{2+}-wave gradient.

We determined whether ectonucleotidases play a role in Ca^{2+} activation by ATP after confirming the presence of ectonucleotidases on MCF-10A cells from previous research (Lawrence *et al.*, 2015; Yu *et al.*, 2017). Because activation depends on ATP and not necessarily from a wound, we performed these assays in a non-wound setting. We used the ectonucleotidase inhibitor ARL67156 at 200 μM, according to literature values, and added a low dose of ATP (0.5 μM; Lévesque *et al.*, 2007). Low concentrations of ATP were used to ensure that cells were not saturated with ATP, making nucleotidase inhibition negligible to the overall response. We found that inhibiting ectonucleotidases did not affect the average Ca^{2+} response (Figure 5A). Because we did not observe a change in Ca^{2+} activation, we further confirmed whether ectonucleotidases influence ATP activation of Ca^{2+} by measuring extracellular phosphate after ATP addition to cells (Figure 5B). Indeed, there is no significant difference in extracellular phosphate concentration in cells perturbed with ATP and without it. In addition, at high levels of ATP (5 μM), we found no difference between ATP and the nonhydrolyzable analogue ATPγS, further supporting that ATP hydrolysis does not play a role in shaping Ca^{2+} activation (Figure 5C)

Amplifying wave: ATP-induced ATP release does not propagate the Ca^{2+} wave

After determining that the Ca^{2+} wave is formed using an extracellular stimulus independent of ATP degradation, we examined whether an amplifying-wave mechanism plays a role in forming the Ca^{2+} wave. That is, does ATP activation initiate the release of ATP to bind extracellular receptors on neighboring cells to propagate the Ca^{2+} response? Prior work suggested that ATP induces the release of additional ATP from cells (ATP-induced ATP release; Locovei *et al.*, 2006; Dubyak, 2009; Corriden and Insel, 2010; Junger, 2011). We first determined whether ATP-induced ATP release is required for ATP-mediated Ca^{2+} activation. We perturbed cells with the nonhydrolyzable ATP variant ATPγS in the presence and absence of the ATP scavenger apyrase (Figure 5C). ATPγS activates a Ca^{2+} response in cells similarly to ATP. In the presence of apyrase, any additional release of ATP is hydrolyzed without affecting ATPγS. Although Ca^{2+} activation by ATPγS in the presence of apyrase shows a statistically significant but small magnitude increase compared with stimulation by ATPγS alone, apyrase does not deplete Ca^{2+} activation in cells when perturbed with ATPγS as it does with ATP. If ATP did induce ATP release, apyrase should deplete Ca^{2+} activation by ATPγS, not increase it; therefore, if an active propagation mechanism exists, cells do not release ATP to activate neighboring cells. The small increase in Ca^{2+} response to ATPγS in the presence of apyrase may be due to other mechanisms not studied here.

Although we saw no evidence for ATP-induced ATP release, it is possible that ATP induces the release of another molecule that propagates the Ca^{2+} wave. We verified the presence of an active release mechanism by measuring the spatial Ca^{2+} activation patterns. Because Ca^{2+} response to wounding is ATP dependent (Figure 3), we simulated wounding using a photoactivated ATP to ensure that we were only measuring Ca^{2+} response according to ATP release and to simplify the measurement (P3-(1-(2-nitrophenyl) ethyl) ester [NPE]-caged ATP; Figure 6). In this assay, ultraviolet (UV) light illumination releases ATP at the site of illumination. We used NPE-caged ATP in combination with a photoactivated fluorescein, bis-(5-carboxymethoxy-2-nitrobenzyl) ether (CMNB)-caged carboxyfluorescein (caged fluorescein isothiocyanate [FITC]), such that the free ATP and free FITC were released in the same area at the same time. We then compared the spatial activation of Ca^{2+} in the surrounding cells with the diffusion pattern of FITC in a flow-free

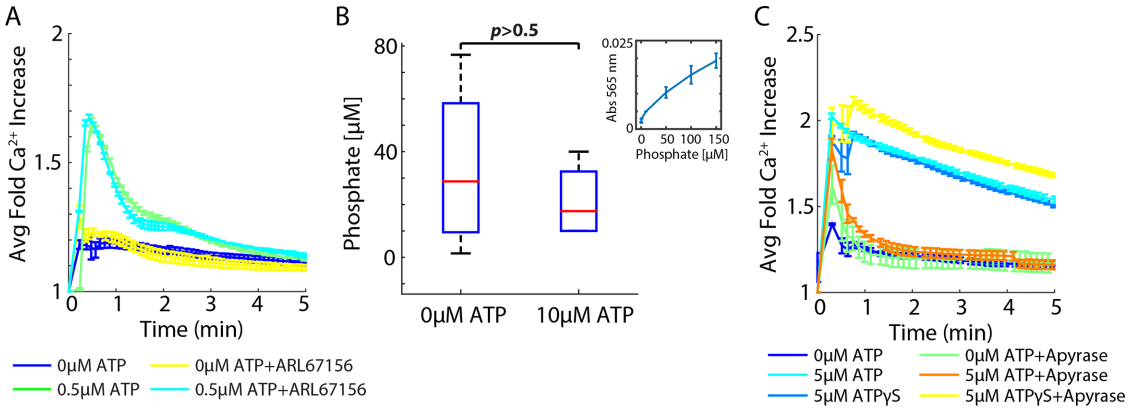

FIGURE 5: Extracellular ATP degradation does not influence Ca^{2+} activation. Ca^{2+} activation measured by genetically encoded biosensor RGECO. (A) Addition of 200 μM ectonucleotidase inhibitor ARL67156 does not increase Ca^{2+} activation by ATP in MCF-10A cells. Error bars indicate SEM, $n = 3$. (B) Extracellular phosphate measurements after the addition of 10 μM ATP show no difference compared with 0 μM. Inset, phosphate standard curve. Error bars indicate SD, $n = 3$, p determined by t test. (C) Ca^{2+} activation by ATP decreases in the presence of the ATP scavenger apyrase (5 U). However, Ca^{2+} activation by the nonhydrolyzable ATP variant ATPγS does not decrease in the presence of apyrase. Error bars indicate SEM, $n = 3$.

environment (Figure 6, A and B). Cells were plated in long Ibidi channels of 400-μm height to capture the full length of response and ensure that released ATP stayed close to the cells. NPE-caged ATP and caged FITC have similar molecular weights (700.3 and 826.8 g/mol, respectively). Therefore the respective molecules have similar diffusion rates. We reasoned that if an active propagation mechanism exists, the spatial distance of Ca^{2+} activation would extend beyond the diffusion pattern of caged FITC. One port of the channel was sealed before uncaging to create a convection-free environment that ensured that any response was not due to flow. However, we found that the Ca^{2+} activation pattern and the caged FITC diffusion pattern were the same in an epithelial monolayer (Figure 6, A and B). This indicates that an active propagation mechanism is not responsible for the Ca^{2+} wave and instead points to a release and diffusion mechanism.

Release and diffusion: ATP passively creates a Ca^{2+} gradient after wounding

The similar patterns created by FITC diffusion and the Ca^{2+} wave indicate that a release and diffusion mechanism might be responsible for Ca^{2+} wave activation. That is, the initial release of ATP from wounded cells diffuses out from the wound to activate neighboring cells. However, other mechanisms might account for these matching patterns. One potential explanation is that ATP interacts with cells (by binding/releasing to/from extracellular receptors) to form an activation pattern similar to diffusion. To determine the presence of an ATP/cellular interaction mechanism, we again used NPE-caged ATP to release ATP from a point source and measured the Ca^{2+} activation patterns over time and space (Figure 6C). To maintain a convection-free environment, we made the NPE-caged ATP solution in a 1% agarose solution that solidified on top of cells before uncaging. In this way, any Ca^{2+} response from ATP would not be due to flow in the well. Measurements were performed in wells to easily add the agarose solution on top of the cells.

We first determined whether Ca^{2+} activation rates changed in the presence (no scratch) or absence (scratch) of cells (Figure 6D). If ATP/cellular interaction took place, then the first response time of cells after the scratch would differ from the response time of cells at the same distance from the site of uncaging without the scratch. Because scratch wounds also elicit a Ca^{2+} response in the neighboring healthy cells, we made the scratch >2 h before the experiment to allow Ca^{2+} levels to reset to normal levels. In addition, we found no difference in Ca^{2+} response between scratched and nonscratched wells after uncaging NPE-caged ATP (unpublished data). We then measured the time of first Ca^{2+} response for each cell after uncaging and quantified the difference in first response times for cells before the scratch (closer to the site of uncaging) and after the scratch (farther from the site of uncaging) to find the difference in Ca^{2+} response times (dT).

We used the same method for cells at similar distances from the uncaging site but without a scratch as an internal control and compared dT for cells with and without a scratch. We found no difference in dT for cells at the same distance from the site of ATP uncaging regardless of the presence or absence of a scratch (Figure 6, E and F, and Supplemental Figure S3). This indicates that ATP does not interact with cells during the spread of the Ca^{2+} wave. Taken together, the results indicate that there is no active mechanism required to form the Ca^{2+}-wave gradient after wounding in an epithelial monolayer of cells. However, the wave is formed using extracellular stimulation. Without an activation mechanism, we next tested whether a simple release and diffusion model explains the propagation of the Ca^{2+} wave. Using our NPE-caged ATP method (Figure 6C), we found the time that each cell first responds to ATP according to its distance from the source (Figure 6G). We then sorted the time for first Ca^{2+} response into bins according to distance from the uncaging site and found that the pattern resembles a square root, similar to the pattern of molecules diffusing from a point source (Figure 6H). Considering the diffusion of ATP from a single point, we fitted our Ca^{2+} response data and calculated a diffusion coefficient of 238.3 (±60.1) $\mu m^2/s$. This closely resembles the reported ATP diffusion coefficient of ~300 $\mu m^2/s$ (Warren *et al.*, 2010).

We conclude that a simple ATP release and diffusion model accounts for the Ca^{2+} wave. In a release and diffusion model, ATP released from wounded cells quickly diffuses from the site of wounding to activate the Ca^{2+} response in surrounding healthy cells in an epithelial monolayer.

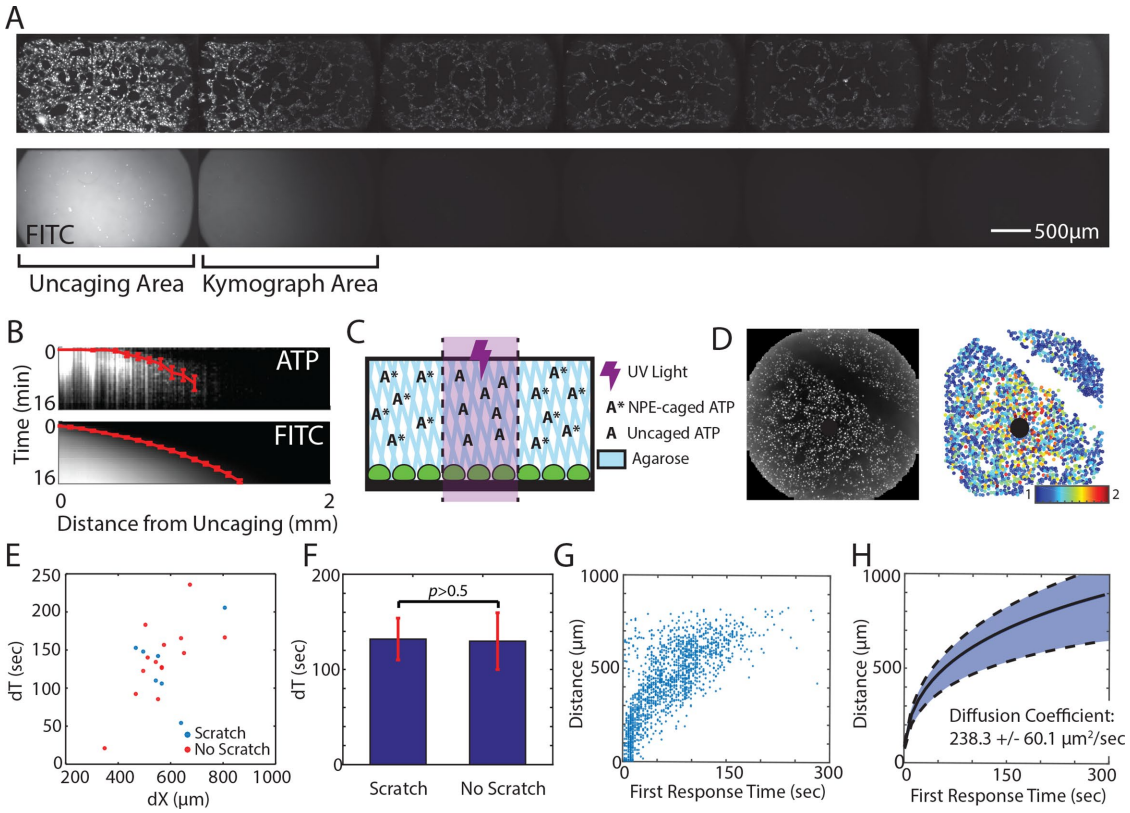

FIGURE 6: The Ca^{2+} wave propagates by ATP diffusion. (A) Photoactivated ATP (NPE-caged ATP) and FITC (CMNB-caged carboxyfluorescein) are uncaged using UV light in the area labeled Uncaging Area. The Ca^{2+} wave, as measured by the genetically encoded biosensor RGECO (top), travels the same distance as uncaged FITC (bottom) in the absence of any flow at 16 min after uncaging. Each side of the channel was taped and allowed to set for 30 min to create a flow-free environment. (B) Kymograph of region indicated in A, showing Ca^{2+} activation and uncaged FITC according to time and distance from uncaging. Red line indicates the average time of first response per binned distance from the uncaging site. Error bars indicate SD of average fluorescence. (C) Spatially activating cells with ATP in a flow-free environment. An NPE-caged ATP solution is made in 1% agarose and added to cells before uncaging. After the agarose has solidified (~10 min), a UV light shines on a specific area of the well to release the caged ATP. This spatial increase of ATP concentration mimics ATP released from a wound source. (D) The time required for the Ca^{2+} wave to cross empty space (scratched) is measured after photoactivated ATP release (black circle). Left, raw maximum projection of Ca^{2+} response (measured by RGECO) in MCF-10A cells. Right, maximum Ca^{2+} projection in which each circle represents a cell and the color indicates fold Ca^{2+} increase (color bar). (E) The time required for the Ca^{2+} wave to cross a specific distance (*dX*) in the presence (no scratch, red) or absence (scratch, blue) of cells is measured by the difference between the time a cell first responds to ATP at the distance further from the uncaging site and the distance closer to the uncaging site (*dT*). (F) The Ca^{2+} wave takes the same amount of time to traverse a specific distance in the presence (no scratch) or absence (scratch) of cells ($p > 0.5$, *t* test, $n = 7$). (G) The distance of each cell according to the time that each cell first shows Ca^{2+} activation above a threshold after ATP uncaging (no scratch). (H) Propagation of the Ca^{2+} wave according to the first response after ATP uncaging follows a pattern best fit by diffusion. The cellular Ca^{2+} response after ATP uncaging from several wells, as in the well shown in G, were averaged for binned distances after ATP release. Data are fitted according to *ATP diffusion fitting* under *Materials and Methods* to find the diffusion coefficient. The diffusion coefficient that best describes the fitted data is 238.3 ± 60.1 $\mu m^2/s$ (SEM, $n = 3$).

DISCUSSION

Here we investigate the underlying mechanism responsible for propagation of Ca^{2+} activation from a wound. Multiple mechanisms have been proposed for wound-induced Ca^{2+} waves (Klepeis *et al.*, 2001, 2004; Yin *et al.*, 2007; Block and Klarlund, 2008; Razzell *et al.*, 2013). These different mechanisms can be classified under three archetypes: source and sink, amplifying wave, and release and diffusion (Figure 1). Evidence from a combination of pharmacological perturbations and quantitative measurements of Ca^{2+} wave propagation contradict key predictions of the amplifying wave and source and sink models. These contradictions suggest that the Ca^{2+} wave propagates via a simple release and diffusion process. Specifically, ATP molecules released from wounded cells diffuse to activate Ca^{2+} in the surrounding healthy cells. The natural dilution of ATP molecules resulting from diffusion forms the Ca^{2+} gradient across space.

Each of the proposed models has features necessary for effective wound response but also comes with key limitations. To initiate a proper wound response, cells need to know 1) the location of the wound and 2) the magnitude of the wound. Neutrophils, macrophages, and epithelial cells use signals indicating the location of the wound in order to find the wound and fight invading pathogens and close the wound. However, this response needs to scale with the magnitude of the wound. A response that is too small results in

ineffective healing. A response that is too large can result in excess scarring and even cancer (Darby and Hewitson, 2007; Eming *et al.*, 2007; Schäfer and Werner, 2008; Feng *et al.*, 2010). In addition, this information must be propagated quickly to begin the wound-healing process. By definition, the source and sink model is self-limiting and ensures that the Ca^{2+} response remains close to the wound. In this model, the response gradient forms when a large amount of initial signal is released (source) and then hydrolyzed spatially (sink). This model tightly regulates the ATP propagation distance. Although this tight regulation is necessary to control the spatial response, it can potentially limit how well the Ca^{2+} response gradient scales with wound size. In contrast to the source and sink model, the amplifying wave model allows Ca^{2+} activation to spread far from the wound source on a realistic time scale. However, signal amplification may result in information loss concerning the magnitude of the wound. Furthermore, although spreading the signals to far distances may be valuable to recruit immune cells, without self-limiting of the wave, the spread of information to distances far from the wound can initiate an undesired inflammatory response. The release and diffusion model contains features desired for a proper wound response mechanism. A release and diffusion model uses ATP molecules released from wounded cells as DAMPs to spread to the surrounding healthy cells. It spreads information on a short time scale, scales with wound size, and is self-limiting to prevent undesired activation of faraway cells. Furthermore, an ATP release and diffusion model is a simple and straightforward mechanism that requires little additional regulation.

Although the three models we investigated here were chosen as representative mechanistic archetypes, it is possible that the overall Ca^{2+} propagation mechanism uses a combination of models. For example, the amplifying wave and source and sink models could be combined to a fourth mechanism that balances the contributions of ATP secretion and hydrolysis. However, our data do not support such a model. Our experiments using a cell gap or "scratch" to measure the rate of Ca^{2+} response spread are independent of the molecular pathway underlying an active propagating wave. In addition, although our results point to a release and diffusion model as the core propagation mechanism, it is possible that amplifying wave or source and sink components act in parallel. Our experimental analysis of Ca^{2+} response propagation did not find any evidence for such parallel mechanisms. If this is the case, any additional components to the core release and diffusion model marginally contribute to Ca^{2+}-wave propagation.

One key limitation to our result is that our experiments were conducted in an in vitro setting. It is possible that more complex mechanisms occur in vivo. However, the lack of complexity in our model is informative and can direct future research in an in vivo context. It is possible that a three-dimensional in vivo model, as opposed to the two-dimensional (2D) monolayer in our system, will result in a different response mechanism. Yet epithelial layers in many organs such as the cornea are very thin and extend to only three cell layers. Therefore our results provide a good approximation of in vivo geometry. Another important consideration is that the multiple cell types required for wound healing will change the Ca^{2+}-wave dynamics and, therefore, the underlying propagation mechanism. Future work quantifying the spatiotemporal dynamics of Ca^{2+} waves in vivo is required to understand how other cell types are involved. It is clear that our model does not capture the full complexity of wound healing in vivo. Yet the simplicity of a release and diffusion model may be beneficial to ensure that surrounding cells are alerted quickly. Future work will determine the extent to which a release and diffusion model plays a role in the complexity of in vivo wound healing.

MATERIALS AND METHODS

Ca^{2+} measurements in MCF-10A cells

MCF-10A cells obtained from the American Type Culture Collection were cultured following established protocols (Debnath *et al.*, 2003). Cells were tested for mycoplasma every 6 mo. Before plating cells, each surface was first treated with a collagen (Life Technologies), bovine serum albumin (New England Biolabs), and fibronectin (Sigma-Aldrich) solution in order for cells to completely adhere, according to established methods. To maintain a viable environment, cells were imaged at 32°C and 5% CO_2. All DREADD experiments were conducted in 96-well plates using extracellular 4-(2-hydroxyethyl)-1-piperazineethanesulfonic acid (HEPES) buffer (ECB) to reduce background fluorescence (5 mM KCl, 125 mM NaCl, 20 mM HEPES, 1.5 mM $MgCl_2$, and 1.5 mM $CaCl_2$, pH 7.4). All wound imaging was done in MCF-10A assay medium (Debnath *et al.*, 2003).

Single-cell Ca^{2+} levels during wounding and DREADD experiments were measured using Fluo-4 AM (F14201; ThermoFisher) to prevent overlap of fluorescence wavelengths of DREADD (mCherry, 587/610 nm), Fluo-4 AM (494/506 nm), and R-GECO (mApple, 568/592 nm). Cells were loaded with 8 μM Fluo-4 AM, 1X PowerLoad (P10020; ThermoFisher), 2.5 mM probenecid (P36400), and 20 μM Hoechst for 30 min at room temperature in ECB. Cells were washed with ECB to remove any remaining extracellular dye. All other Ca^{2+} measurements were conducted using the genetically encoded fluorescent biosensor R-GECO (Zhao *et al.*, 2011; Akerboom *et al.*, 2013).

Wounding-device design and fabrication and wounding assay

Master molds for the microfluidics-based wounding device were created using silicon wafers and layer-by-layer photolithography using established methods (Ferry *et al.*, 2011). Separate molds for the air layer and cell layer were made using negative photoresists and masks. Chips were made by pouring uncured polydimethylsiloxane (PDMS) onto each mold, allowing the PDMS to harden, and bonding the layers together and subsequently to a glass slide. Cells were loaded into the device through the inlet port using a 20-gauge needle. During wounding, the outlet port was plugged using tape, and the inlet port held a reservoir of medium to prevent evaporation in the chamber. Wounding was accomplished by increasing the air pressure in the top layer of the device until the pillar made contact with the bottom of the device, after which the air pressure was released to raise the pillar back up. Cells were loaded in to the wounding device at a density of 15 million cells/ml using a 20-gauge needle. After trypsinization and resuspension, cells were put on ice to prevent aggregation. Two O-rings were attached to the device surrounding both the inlet and outlet ports for media reservoirs using a thin film of vacuum grease. Wounding devices were kept in an empty pipette box filled with water to prevent media evaporation. Cells were allowed to adhere for 18–24 h before wounding.

Ca^{2+} activation by DREADD

Cells were plated at a density of 2 million cells/100-mm plate and allowed to adhere overnight. Cells were transfected with the Gq-coupled DREADD hemagglutinin-tagged hM3D with an mCherry tag using a 3:1 ratio of FuGENE HD (Promega) to DNA and allowed to incubate overnight (Dong *et al.*, 2010). To measure the effect of activating a single cell, nontransfected cells were mixed with DREADD-transfected cells at ratios of 1:0, 1:1, 1:2, 1:5, 1:7, and 0:1 (nontransfected:DREADD) and plated in 96-well plates at a density of 30,000 cells/well. The next day, cells were loaded with 1 μM

Hoechst dye for nuclear imaging for 30 min for cell segmentation purposes and Fluo-4 AM to measure Ca^{2+} response. CNO at 5 µM (Enzo Life Sciences) was added to each well to specifically activate DREADD cells.

Manipulating extracellular ATP levels

Two methods were used to manipulate extracellular ATP: 1) inhibition of ectonucleotidases with ARL67156 and 2) ATP hydrolysis with apyrase. Cells were plated in 96-well plates at a density of 30,000 cells/well and allowed to adhere overnight. Cells were incubated with 200 µM ARL67156 for 1 h, after which 0.5 µM of ATP was added to the well. Extracellular ATP was hydrolyzed by adding 5 U of apyrase (A7646; Sigma-Aldrich) to the well before addition of 5 µM ATP or ATPγS (4080; Tocris). In the wounding device, 5 U of apyrase was added to the inlet port just before sealing off of the second port to ensure that the apyrase stayed in the cell chamber. Cells were imaged in FluoBrite DMEM (A1896701; ThermoFisher) with the components necessary for MCF-10A assay medium added.

Extracellular phosphate measurement

Extracellular phosphate was measured using the PiPer Phosphate Assay Kit (P22061; Thermo Fisher) using the provided protocol. Cells were perturbed with either 0 or 10 µM ATP and allowed to sit for 5 min to capture full Ca^{2+} activation. A portion of the medium was taken from the wells and used for the PiPer phosphate assay. Absorbance was measured on a plate reader at 565 nm.

Spatial measurements of the Ca^{2+} wave

MCF-10A cells were plated in coated Ibidi µ-Slide VI$^{0.1}$ chips by adding 20 µl of a cellular solution with a density of 1×10^6 cells/ml to each channel of the µ-Slide. Cells were allowed to settle for 1 h, after which each well was filled with MCF-10A assay medium (Debnath *et al.*, 2003). Cells were allowed to adhere overnight. To measure the distance of Ca^{2+} wave response, we used 1 mM NPE-caged ATP (A1048; ThermoFisher) and 10 mM CMNB-caged fluorescein (F7103; ThermoFisher). NPE-caged ATP and CMNB-caged fluorescein were uncaged in specific regions by shining UV light on the region for 20 s. Enough NPE-caged ATP solution was added to the channel to partially fill each well. Each well was taped and allowed to sit for >30 min to stop flow through the channel.

All other NPE-caged ATP experiments were done in a 96-well plate in an agarose solution to prevent any convection during uncaging and imaging. NPE-caged ATP solutions were made in a 1% agarose solution and allowed to solidify for 10 min at room temperature before uncaging. Each well was exposed with UV light for 10 s to uncage NPE-caged ATP. To determine whether the Ca^{2+} wave could cross empty space, cells were seeded in a 96-well plate at a density of 30,000 cells/well and allowed to adhere overnight. Cell monolayers were scratched using a 2-µl pipette tip to create empty space. Scratches were done >4 h before imaging to give Ca^{2+} levels adequate time to return to basal levels. A 1% agarose solution containing 10 µM NPE-caged ATP was added to each well and allowed to solidify for 10 min at room temperature. Each well was exposed to UV light for 10 s to uncage NPE-caged ATP.

ATP diffusion fitting

We considered the diffusion of ATP from a single point to its surrounding neighbors to find the diffusion coefficient, D, of the molecule responsible for Ca^{2+} wave propagation after ATP release. We considered a 2D-like geometry in which cylindrical cells, each of height h_c and radius ρ, grow in a chamber of total height h_f. We simplify the following analysis by approximating the cell monolayer geometry by a series of cell cylinders. We also consider the number of molecules released from a cell, N_r, the number of molecules needed for detection N_d, and the total integration time, T. The key results of the required integration time are similar for other comparable geometries (unpublished data). Under these conditions, we can write the analytical solution of the diffusion equations,

$$C(r,t) = \frac{N_r}{h_f \cdot 4D\pi t} e^{-\frac{r^2}{4Dt}} \quad (1)$$

where $C(r, t)$ is the concentration of ATP for distance r and time t. For a neighboring cell to respond to this paracrine signal, a critical number of molecules, N_d, need to reach the volume surrounding the cell. We assume that a cell "senses" a volume comparable to the volume of the cell itself. For a cylindrical cell of area $\pi\rho^2$ and height h_c, the critical concentration required for cellular response is

$$C_{detect} = \frac{N_d}{h_c \pi \rho^2} \quad (2)$$

This is simply the required number of molecules divided by the cell volume. Combining Eqs. 1 and 2, we can solve for the distance and time of where the critical concentration will be reached. Solving for distance, we get

$$r_{detect} = 2\sqrt{Dt \ln\left(\frac{\rho^2 h_c N_r}{4DtN_d h_f}\right)} \quad (3)$$

Using the time of first response for each cell with its corresponding distance from the ATP source, we used Eq. 3 to fit the experimental data to get the ATP diffusion coefficient.

Imaging and image analysis

Imaging was accomplished using a Nikon Plan Apo λ 10×/0.45 objective with a 0.7× demagnifier and Nikon Eclipse Ti microscope with a scientific complementary metal-oxide-semiconductor Zyla camera. All imaging was done using custom automated software written using MATLAB and Micro-Manager (Edelstein *et al.*, 2010). Image analysis was done using a previously published custom MATLAB code (Selimkhanov *et al.*, 2014; Supplemental Figure S4)

ACKNOWLEDGMENTS

The work was supported by National Institutes of Health R01-GM111404 and R01-EY024960 (R.W.) and National Institutes of Health training grant T32-GM007240 (L.N.H.).

REFERENCES

Akerboom J, Carreras Calderón N, Tian L, Wabnig S, Prigge M, Tolö J, Gordus A, Orger MB, Severi KE, Macklin JJ, *et al.* (2013). Genetically encoded calcium indicators for multi-color neural activity imaging and combination with optogenetics. Front Mol Neurosci 6, 2.

Armbruster BN, Li X, Pausch MH, Herlitze S, Roth BL (2007). Evolving the lock to fit the key to create a family of G protein-coupled receptors potently activated by an inert ligand. Proc Natl Acad Sci USA 104, 5163–5168.

Berridge MJ, Lipp P, Bootman MD (2000). The versatility and universality of calcium signalling. Nat Rev Mol Cell Biol 1, 11–21.

Block ER, Klarlund JK (2008). Wounding sheets of epithelial cells activates the epidermal growth factor receptor through distinct short- and long-range mechanisms. Mol Biol Cell 19, 4909–4917.
Block ER, Matela AR, SundarRaj N, Iszkula ER, Klarlund JK (2004). Wounding induces motility in sheets of corneal epithelial cells through loss of spatial constraints: role of heparin-binding epidermal growth factor-like growth factor signaling. J Biol Chem 279, 24307–24312.
Bootman MD (2012). Calcium signaling. Cold Spring Harb Perspect Biol 4, a011171.
Caporossi A, Manetti C (1992). Epidermal growth factor in topical treatment following epikeratoplasty. Ophthalmologica 205, 121–124.
Cordeiro JV, Jacinto A (2013). The role of transcription-independent damage signals in the initiation of epithelial wound healing. Nat Rev Mol Cell Biol 14, 249–262.
Corriden R, Insel PA (2010). Basal release of ATP: an autocrine-paracrine mechanism for cell regulation. Sci Signal 3, re1.
Debnath J, Muthuswamy SK, Brugge JS (2003). Morphogenesis and oncogenesis of MCF-10A mammary epithelial acini grown in three-dimensional basement membrane cultures. Methods 30, 256–268.
Dong S, Allen JA, Farrell M, Roth BL (2010). A chemical-genetic approach for precise spatio-temporal control of cellular signaling. Mol Biosyst 6, 1376–1380.
Dubyak GR (2009). Both sides now: multiple interactions of ATP with pannexin-1 hemichannels. Focus on "A permeant regulating its permeation pore: inhibition of pannexin 1 channels by ATP". Am J Physiol Cell Physiol 296, C235–C241.
Dupont G (2014). Modeling the intracellular organization of calcium signaling. WIRES Syst Biol Med 6, 227–237.
Edelstein A, Amodaj N, Hoover K, Vale R, Stuurman N (2010). Computer control of microscopes using μManager. Curr Protoc Mol Biol Chapter 14, Unit 14.20.
Eming SA, Krieg T, Davidson JM (2007). Inflammation in wound repair: molecular and cellular mechanisms. J Invest Dermatol 127, 514–525.
Enyedi B, Niethammer P (2015). Mechanisms of epithelial wound detection. Trends Cell Biol 25, 398–407.
Feldman S (1991). The effect of epidermal growth factor on corneal wound healing: practical considerations for therapeutic use. Refract Corneal Surg 7, 232–239.
Feng Y, Santoriello C, Mione M, Hurlstone A, Martin P (2010). Live imaging of innate immune cell sensing of transformed cells in zebrafish larvae: parallels between tumor initiation and wound inflammation. PLoS Biol 8, e1000562.
Ferry MS, IA Razinkov, Hasty J (2011). Microfluidics for synthetic biology: from design to execution. Methods Enzymol 497, 295–372.
Gault WJ, Enyedi B, Niethammer P (2014). Osmotic surveillance mediates rapid wound closure through nucleotide release. J Cell Biol 207, 767–782.
Handly LN, Pilko A, Wollman R (2015). Paracrine communication maximizes cellular response fidelity in wound signaling. Elife 4, 1–18.
Ho C-L, Yang C-Y, Lin W-J, Lin C-H (2013). Ecto-nucleoside triphosphate diphosphohydrolase 2 modulates local ATP-induced calcium signaling in human HaCaT keratinocytes. PLoS One 8, e57666.
Höfer T, Politi A, Heinrich R (2001). Intercellular Ca2+ wave propagation through gap-junctional Ca2+ diffusion: a theoretical study. Biophys J 80, 75–87.
Darby IA, Hewitson TD (2007). Fibroblast differentiation in wound healing and fibrosis. Int Rev Cytol 257, 143–179.
Idzko M, Ferrari D, Eltzschig HK (2014). Nucleotide signalling during inflammation. Nature 509, 310–317.
Junger WG (2011). Immune cell regulation by autocrine purinergic signalling. Nat Rev Immunol 11, 201–212.
Klarlund JK, Block ER (2011). Free edges in epithelia as cues for motility. Cell Adhes Migr 5, 106–110.
Klepeis VE, Cornell-Bell A, Trinkaus-Randall V (2001). Growth factors but not gap junctions play a role in injury-induced Ca 2+ waves in epithelial cells. J Cell Sci 114, 4185–4195.
Klepeis VE, Weinger I, Kaczmarek E, Trinkaus-Randall V (2004). P2Y receptors play a critical role in epithelial cell communication and migration. J Cell Biochem 93, 1115–1133.
Lawrence RT, Perez EM, Blau CA, Miller CP, Haas KM, Irie HY, Lawrence RT, Perez EM, Herna D (2015). The proteomic landscape of triple-negative breast resource the proteomic landscape of triple-negative breast cancer. Cell Rep 11, 630–644.
Lévesque SA, Lavoie EG, Lecka J, Bigonnesse F, Sévigny J (2007). Specificity of the ecto-ATPase inhibitor ARL 67156 on human and mouse ectonucleotidases. Br J Pharmacol 152, 141–150.
Locovei S, Wang J, Dahl G (2006). Activation of pannexin 1 channels by ATP through P2Y receptors and by cytoplasmic calcium. FEBS Lett 580, 239–244.
Nakagawa S, Omura T, Yonezawa A, Yano I, Nakagawa T, Matsubara K (2014). Extracellular nucleotides from dying cells act as molecular signals to promote wound repair in renal tubular injury. Am J Physiol Renal Physiol 307, F1404–F1411.
Pastor J, Calonge M (1992). Epidermal growth factor and corneal wound healing. A multicenter study. Cornea 11, 311–314.
Razzell W, Evans IR, Martin P, Wood W (2013). Calcium flashes orchestrate the wound inflammatory response through DUOX activation and hydrogen peroxide release. Curr Biol 23, 424–429.
Schäfer M, Werner S (2008). Cancer as an overhealing wound: an old hypothesis revisited. Nat Rev Mol Cell Biol 9, 628–638.
Schwiebert EM, Zsembery A (2003). Extracellular ATP as a signaling molecule for epithelial cells. Biochim Biophys Acta 1615, 7–32.
Selimkhanov J, Taylor B, Yao J, Pilko A, Albeck J, Hoffmann A, Tsimring L, Wollman R (2014). Accurate information transmission through dynamic biochemical signaling networks. Science 346, 1370–1373.
Sonnemann KJ, Bement WM (2011). Wound repair: toward understanding and integration of single-cell and multicellular wound responses. Annu Rev Cell Dev Biol 27, 237–263.
Sun B, Lembong J, Normand V, Rogers M, Stone HA (2012). Spatial-temporal dynamics of collective chemosensing. Proc Natl Acad Sci USA 109, 7753–7758.
Takada H, Furuya K, Sokabe M (2014). Mechanosensitive ATP release from hemichannels and Ca^{2+} influx through TRPC6 accelerate wound closure in keratinocytes. J Cell Sci 127, 4159–4171.
Warren NJ, Tawhai MH, Crampin EJ (2010). Mathematical modelling of calcium wave propagation in mammalian airway epithelium: evidence for regenerative ATP release. Exp Physiol 95, 232–249.
Wesley UV, Bove PF, Hristova M, McCarthy S, van der Vliet A (2007). Airway epithelial cell migration and wound repair by ATP-mediated activation of dual oxidase 1. J Biol Chem 282, 3213–3220.
Yin J, Xu K, Zhang J, Kumar A, Yu F-SX (2007). Wound-induced ATP release and EGF receptor activation in epithelial cells. J Cell Sci 120, 815–825.
Yu J, Liao X, Li L, Lv L, Zhi X, Yu J, Yu J (2017). A preliminary study of the role of extracellular -5 ′-nucleotidase in breast cancer stem cells and epithelial-mesenchymal transition, In Vitro Cell Dev Biol Anim 53, 132–140.
Zhao Y, Araki S, Wu J, Teramoto T, Chang YF, Nakano M, Abdelfattah AS, Fujiwara M, Ishihara T, Nagai T, Campbell RE (2011). An expanded palette of genetically encoded Ca^{2+} indicators. Science 333, 1888–1891.